Aeroelastic Analysis of Composite Pinched Panels using Higher-Order Shell Elements

JOURNAL OF SPACECRAFT AND ROCKETS
Vol. , No. ,

# Engineering Notes

## Aeroelastic Analysis of Composite Pinched Panels Using Higher-Order Shell Elements

E. Zappino,* E. Carrera,† and M. Cinefra‡
*Politecnico di Torino, Corso Duca degli Abruzzi 24, 10129 Torino, Italy*

DOI: 10.2514/1.A32986

### I. Introduction

AEROELASTIC phenomena are increasingly important in the analysis of aeronautical and space structures. They can sometimes involve only one component of the structure. Panels are a typical example: they are usually subjected to high aerodynamic loads and can be afflicted by a dangerous aeroelastic phenomenon called *panel flutter*. Panel flutter was observed for the first time when the first supersonic flights were performed and it was studied theoretically in the fifties by Hayes [1], Miles [2], and Shen [3]. Significant contributions have been made by Dowell [4–6]. The classical approach to panel flutter analysis considers both the aerodynamic and the structural model as linear. The fluid is usually approximated via the "piston theory" proposed by Ashley and Zartarian [7], while the structural model uses classical approaches such as plate and shell models [8].

Refined structural models are required when non-classical configurations are considered. The effects of thermal [9] and in-plane [10] loads can be considered as well as the use of anisotropic, layered and composite materials as shown in the works by Shiau and Lu [11], Dixon and Mei [12], and Kouchakzadeh et al. [13]. The use of advanced aerodynamic models allows the analysis to be extended to larger Mach number regimes, as shown by Gordiner and Visbal [14] and Hashimoto et al. [15]. Advanced structures such as the thermal insulation panels used in launcher structures are larger than common aeronautical panels; these are usually connected to the main structure by means of pinched points. Their features make these panels very flexible and therefore they could be affected by aeroelastic phenomena. In the works by Carrera and Zappino [16] and Carrera et al. [17,18], a refined one-dimensional structural model was used to analyze the aeroelastic behaviour of such panels.

In the present paper, the effects of unconventional boundary conditions and of advanced composite materials on panel flutter are investigated. A refined shell model originally introduced by Cinefra and Carrera [19] is extended to the aeroelastic formulation to overcome the limitation of the classical models. The structural model is based on the Carrera Unified Formulation, CUF, which allows any model to be derived with a unified and compact formulation. The theoretical foundations of the method can be found in Carrera et al. [20]. Both equivalent single layer (ESL) and layer-wise (LW) models are considered. The solution is obtained via finite element method (FEM) using a 9-node element based on the MITC9 formulation [21]. The fluid model is based on the linear formulation of the piston theory, therefore only supersonic regimes are investigated. Where possible, the results are compared with those from the one-dimensional model presented in [16].

Received 12 March 2014; revision received 19 September 2014; accepted for publication 12 October 2014; published online XX epubMonth XXXX. 

*Research Assistant, Department of Mechanical and Aerospace Engineering; enrico.zappino@polito.it.
†Professor of Aerospace Structures and Aeroelasticity, Department of Mechanical and Aerospace Engineering; also Faculty of Science, King Abdulaziz University, Jeddah, Saudi Arabia; erasmo.carrera@polito.it. Member AIAA (Corresponding Author).
‡Research Assistant, Department of Mechanical and Aerospace Engineering; maria.cinefra@polito.it.

### II. Aeroelastic Model

The aeroelastic model can be written using the Principle of Virtual Displacements:

$$\delta L_{\text{int}} + \delta L_{\text{ine}} = \delta L_{\text{ext}} \tag{1}$$

where $L_{\text{int}}$ is the internal virtual work due to the elastic forces, $L_{\text{ine}}$ is the work due to the inertial forces, and $L_{\text{ext}}$ is the work due to the external forces. $\delta$ denotes virtual variations. Using FEM, Eq. (1) can be written in matrix form:

$$([\boldsymbol{K}] + [\boldsymbol{K}_a])\{\boldsymbol{q}\} + ([\boldsymbol{D}_a])\{\dot{\boldsymbol{q}}\} + ([\boldsymbol{M}])\{\ddot{\boldsymbol{q}}\} = 0 \tag{2}$$

where $[\boldsymbol{K}]$ is the stiffness matrix, $[\boldsymbol{M}]$ is the mass matrix, $[\boldsymbol{K}_a]$ is the aerodynamic stiffness matrix, and $[\boldsymbol{D}_a]$ is the aerodynamic damping matrix.

#### A. Advanced Shell Elements

The refined shell model used in the present paper is derived using CUF [22]. As in any shell theory the generic three-dimensional displacement field can be expressed as a contribution on the reference surface and a contribution on the thickness. The displacement field therefore assumes the following form:

$$\boldsymbol{u}^k(\alpha,\beta,z) = F_\tau(z) N_i(\alpha,\beta)\boldsymbol{q}^k_{i\tau} \;\; \tau = 1,\ldots,N; \;\; i = 1,\ldots,N_n \tag{3}$$

where $(\alpha,\beta,z)$ is the curvilinear reference system shown in Fig. 1 and $k$ identifies the generic layer. $F_\tau$ is a function which depends only on $z$ and is used to approximate the deformation through the thickness of the shell. The choice of $F_\tau$ is discussed below and $\tau$ is the number of terms in the expansion. $N_i$ are the Lagrangian shape functions introduced by the FEM formulation.

Two different approaches are used in the thickness approximation: ESL and LW approximation. In the case of ESL models, a Taylor expansion is employed in the thickness direction. In this work, these models are indicated with the acronym $ED-N$ where $N$ is the number of terms of the expansion. In the case of LW models, the displacement is defined at layer level. These models are denoted using $LD-N$ where $N$ is the number of terms of the expansion in each layer. The LW models allow the zig-zag form of the displacement distribution in layered structures to be modelled, while the ESL models would require some improvements, the Murakami zig-zag functions, to provide an accurate displacement distribution. More details can be found in Cinefra et al. [21] and in Carrera et al. [20].

The internal work, $\delta L_{\text{int}}$, can be expressed in terms of elastic energy using the equations introduced in the section above:

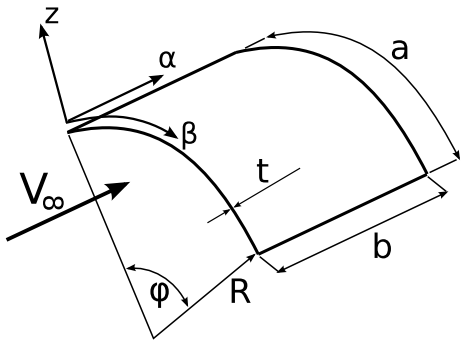


**Fig. 1 Geometry and reference system.**

$$\begin{aligned}\delta L_{\text{int}} &= \int_V \delta\boldsymbol{\varepsilon}^T\boldsymbol{\sigma}\,\mathrm{d}V \\ &= \delta\mathbf{q}_{\tau i}^{kT}\left[\int_V \boldsymbol{D}^T(N_i(\alpha,\beta)F_\tau(z)\boldsymbol{I})\boldsymbol{C}^k(N_j(\alpha,\beta)F_s(z)\boldsymbol{I})\boldsymbol{D}\,\mathrm{d}V\right]\mathbf{q}_{sj}^k \\ &= \delta\mathbf{q}_{\tau i}^{kT}\mathbf{k}^{kij\tau s}\mathbf{q}_{sj}^k \end{aligned} \tag{4}$$

where $\boldsymbol{C}$ is the material coefficients matrix and $\boldsymbol{D}$ is a differential operator matrix used to derive the strains from the displacements. The mass matrix is derived from the variation of the work made by the inertial forces:

$$\begin{aligned}\delta L_{\text{ine}} &= \int_V \delta\mathbf{u}\,\ddot{\mathbf{u}}\rho^k\,\mathrm{d}V \\ &= \delta\mathbf{q}_{i\tau}^{kT}\left[\int_V (F_\tau(z)\boldsymbol{I}\cdot N_i(\alpha,\beta)\cdot N_j(\alpha,\beta)\cdot F_s(z)\boldsymbol{I}\cdot\rho^k)\,\mathrm{d}V\right]\ddot{\mathbf{q}}_{sj}^k \\ &= \delta\mathbf{q}_{i\tau}^{kT}\mathbf{m}^{kij\tau s}\ddot{\mathbf{q}}_{sj}^k \end{aligned} \tag{5}$$

Double dot denotes acceleration. The explicit form of stiffness matrix and the mass matrix can be found in Carrera et al. [22].

### B. Aerodynamic Model

The aerodynamic model is based on the Piston Theory presented by Ashley and Zartarian [7]. The piston theory assumes that the flow on a panel is similar to a one-dimensional flow in a channel (e.g., in a piston). The pressure distribution can be expressed as:

$$\Delta p(y,t) = \frac{2\lambda}{\sqrt{M^2-1}}\left\{\frac{\partial u_z}{\partial\alpha} + \frac{M^2-2}{M^2-1}\frac{1}{V_\infty}\frac{\partial u_z}{\partial t}\right\} \tag{6}$$

where the flow parameters are the Mach number, $M$, the flow velocity, $V_\infty$, and the dynamic pressure, $\lambda$. $u_z$ is the component of the displacement in $z$-direction while $\alpha$ denotes the longitudinal direction, in accordance with Fig. 1. The aerodynamic stiffness matrix can be derived by evaluating the work, $\delta L_{\text{aer}}$, made by a differential pressure, $\Delta p$, on the reference surface, $\Omega$, due to the slope of the surface in the flow direction.

$$\boldsymbol{k}_a^{kij\tau s} = \frac{2\lambda}{\sqrt{M^2-1}}F_\tau F_s|_z\begin{bmatrix}0 & 0 & 0\\ 0 & 0 & 0\\ 0 & 0 & \int_\Omega N_j\frac{\partial N_i}{\partial\alpha}\,\mathrm{d}\Omega\end{bmatrix} \tag{7}$$

To notice that $\mathrm{d}\Omega = \mathrm{d}\alpha\cdot\mathrm{d}\beta$. The aerodynamic damping matrix can be derived by evaluating the work, $\delta L_{\text{aer}}$, made by a differential pressure, $\Delta p$, due to the vertical velocity of the surface.

$$\boldsymbol{d}_a^{kij\tau s} = \frac{2\lambda}{\sqrt{M^2-1}}\frac{1}{V_\infty}\left(\frac{M^2-2}{M^2-1}\right)F_\tau F_s|_z\begin{bmatrix}0 & 0 & 0\\ 0 & 0 & 0\\ 0 & 0 & \int_\Omega N_i N_j\,\mathrm{d}\Omega\end{bmatrix} \tag{8}$$

## III. Numerical Results Analysis

This section shows the performances of the present refined shell model and the impact of higher-order models on the aeroelastic analysis. Different panel configurations are investigated. The effects of non-conventional boundary conditions, lamination, sandwich material and curvature are considered.

### A. Convergence Analysis and Assessment

Eight meshes were considered, from $2\times2$ to $9\times9$ elements. Two panels were investigated: a simply supported (SS) flat plate with dimensions $b = 0.5$ m and $a = 1$ m and a square flat panel pinched supported (PPPP) at the four corners with dimensions $a = b = 0.5$ m. Both models had a thickness of 0.002 m and they were built with an aluminium alloy: $E = 73$ GPa, $\nu = 0.3$, and a density of $\rho = 2700$ kg/m$^3$. An ED2 structural model was used in both cases. The flow parameters were derived according to the standard atmosphere model. The first panel was analysed at an altitude of 11,000 m while the second at 20,000 m. These altitudes would permit flutter at supersonic speed by preserving the validity of the used piston-theory. Table 1 shows the results of the FEM convergence analysis. The SS model needs a rather coarse mesh to achieve very good convergence ($3\times3$ mesh) while the PPPP models converge only with a $9\times9$ mesh, although the solution with a $5\times5$ mesh is quite close to the reference model.

The aeroelastic model based on refined structural theories was assessed comparing the results with those by Krause [23]. The PPPP model described above was used. Both the ESL and LW models were considered as well as expansions of first, second and third order. A $6\times6$ mesh was used for both models. Table 2 shows the results in terms of critical Mach number and flutter frequency. All the models provide good results and are comparable with the reference model.

### B. Number of Pinched Point Effects

The effect of the number of the pinched points on the flutter boundary is investigated in this section. The results are compared with those obtained by the authors in the work [16]. A square panel ($a = b = 0.5$ m) with thickness of 0.002 m is considered, where the material had $E = 75$ GPa, $\nu = 0.3$, and the density was 2700 kg/m$^3$. No displacements or rotations were allowed in the pinched points. The Mach number was fixed to 3.0, the temperature at 216 K and the critical value of density ($\rho_{\text{cr}}$) was investigated. Different numbers of pinched points and different structural models were considered. A $6\times6$ mesh was adopted.

The results are reported in Table 3. As the number of pinched points is increased the critical density values also increase, while the structural model does not have much impact on the results, so classical models can be considered accurate. The results for the fully clamped panel show non-physical values of $\rho_{\text{cr}}$. This means that, for this configuration, flutter cannot appear in the real atmosphere.

The results computed using an LD4 model are compared with those from [16] in Fig. 2. The critical condition evaluated using the shell model appears earlier than those of the one-dimensional model.

**Table 1 Critical Mach number for different FEM discretizations and boundary conditions, model used: ED2**

| MESH | $2\times2$ | $3\times3$ | $4\times4$ | $5\times5$ | $6\times6$ | $7\times7$ | $8\times8$ | $9\times9$ |
|---|---|---|---|---|---|---|---|---|
| SS | 4.91 | 4.39 | 4.39 | 4.39 | 4.39 | 4.39 | 4.39 | 4.39 |
| PPPP | 17.98 | 4.23 | 3.98 | 3.86 | 3.79 | 3.73 | 3.67 | 3.67 |

**Table 2 Effect of the structural model on the aeroelastic solution**

| | [23] | ED2 | ED3 | ED4 | LD2 | LD3 | LD4 |
|---|---|---|---|---|---|---|---|
| Critical M | 4.5 | 4.39 | 4.36 | 4.36 | 4.36 | 4.36 | 4.36 |
| Flutter Freq. | 66.03 | 65.46 | 65.31 | 65.31 | 65.31 | 65.32 | 65.32 |

The results are compared with those from [23].

**Table 3 Critical density value for a square panel with different number of pinched points at M equal to 3**

| | $\rho_{cr}$, Kg/m$^3$ | | | | |
|---|---|---|---|---|---|
| MODEL | ED2 | ED4 | LD2 | LD3 | LD4 |
| P-P | 0.111 | 0.111 | 0.111 | 0.111 | 0.111 |
| P-P | 0.586 | 0.578 | 0.586 | 0.578 | 0.579 |
| P-P | 1.059 | 1.084 | 1.059 | 1.085 | 1.085 |
| Clamped | 1.424 | 1.453 | 1.424 | 1.453 | 1.453 |

This is due to the higher flexibility of the two-dimensional shell formulation.

### C. Tailoring of Composite Panel

The tailoring effects on the aeroelastic instability due to the variation of lamination angle is investigated in this section. The geometry of the panel is the same as that used in Sec. III.B. Different boundary condition configurations were considered, that is, 4 and 8 pinched points. A three-layer orthotropic material was used and the thickness of the layers was $0.0005/0.001/0.0005$ m. The lamination sequence was set equal to $0/\theta/0$, therefore only the middle layer has a variable lamination angle, $\theta$. The analyses were performed with the flow parameters according to the standard atmosphere model at 20,000 m.

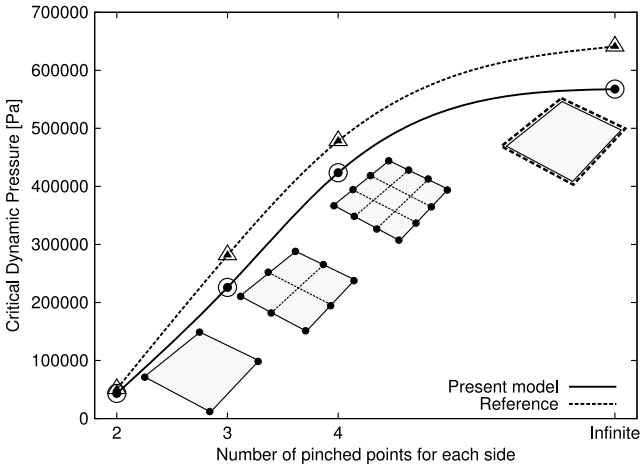


**Fig. 2 Effects of the number of pinched points on the critical dynamic pressure, defined as $\lambda_{cr} = \frac{1}{2}\rho_{cr}V^2$. The present results, evaluated by LD4 model, are compared with those from [16].**

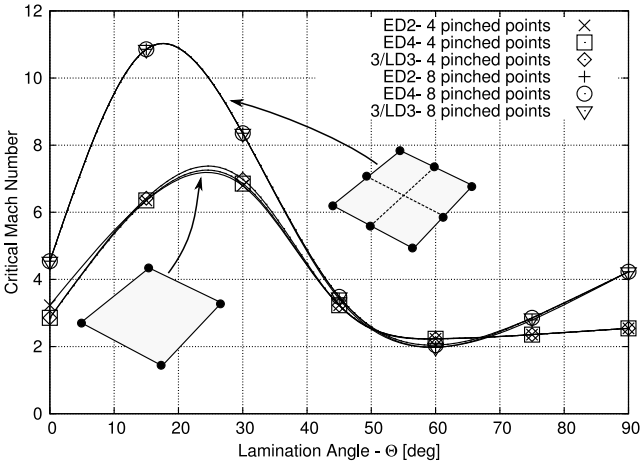


**Fig. 3 Tailoring effects: evolution of the critical Mach number with the lamination angle.**

**Table 4 Effects of the lamination angle on the critical Mach number**

| | | Lamination angle Θ, deg | | | | | | |
|---|---|---|---|---|---|---|---|---|
| | Model | 0 | 15 | 30 | 45 | 60 | 75 | 90 |
| ED2 | 4 P-P | 3.231 | 6.356 | 6.794 | 3.231 | 2.231 | 2.356 | 2.544 |
| ED4 | 4 P-P | 2.856 | 6.356 | 6.856 | 3.231 | 2.231 | 2.356 | 2.544 |
| LD3 | 4 P-P | 2.856 | 6.356 | 6.919 | 3.231 | 2.231 | 2.356 | 2.544 |
| ED2 | 8 P-P | 4.544 | 10.856 | 8.356 | 3.419 | 1.981 | 2.794 | 4.231 |
| ED4 | 8 P-P | 4.544 | 10.856 | 8.356 | 3.481 | 2.044 | 2.856 | 4.231 |
| LD3 | 8 P-P | 4.544 | 10.856 | 8.356 | 3.481 | 1.981 | 2.856 | 4.231 |

4 and 8 pinched point panels are considered. Different structural models are compared.

**Table 5 Effect of the structural model on the first ten natural frequencies for sandwich panel**

| Mode | ED2 | ED4 | LD3 | LD4 |
|---|---|---|---|---|
| 1 | $43.33^{(3.4\%)}$ | $42.51^{(1.4\%)}$ | $41.92^{(0.0\%)}$ | 41.92 |
| 2 | $88.46^{(10.2\%)}$ | $82.33^{(2.5\%)}$ | $80.30^{(0.0\%)}$ | 80.30 |
| 3 | $88.46^{(10.2\%)}$ | $82.33^{(2.5\%)}$ | $80.30^{(0.0\%)}$ | 80.30 |
| 4 | $110.32^{(10.5\%)}$ | $101.45^{(1.6\%)}$ | $99.85^{(0.0\%)}$ | 99.85 |
| 5 | $203.79^{(13.6\%)}$ | $185.88^{(3.6\%)}$ | $179.36^{(0.0\%)}$ | 179.36 |
| 6 | $213.54^{(9.6\%)}$ | $199.53^{(2.4\%)}$ | $194.85^{(0.0\%)}$ | 194.85 |
| 7 | $256.08^{(10.9\%)}$ | $236.50^{(2.5\%)}$ | $230.83^{(0.0\%)}$ | 230.83 |
| 8 | $256.08^{(10.9\%)}$ | $236.50^{(2.5\%)}$ | $230.83^{(0.0\%)}$ | 230.83 |
| 9 | $347.53^{(12.4\%)}$ | $316.53^{(2.4\%)}$ | $309.19^{(0.0\%)}$ | 309.19 |
| 10 | $388.25^{(13.6\%)}$ | $352.83^{(3.3\%)}$ | $341.64^{(0.0\%)}$ | 341.64 |

Table 4 shows the results, in terms of critical Mach number, of three different models: ED3, ED4, and LD3. Different values of $\theta$ are considered: 0, 15, 30, 45, 60, 75, and 90. The same results are reported in Fig. 3. They show that lamination can play an important role in the aeroelastic phenomena. Figure 3 shows a maximum critical condition for a lamination angle close to 20 deg, and a minimum for $\theta$ close to 60 deg for both the boundary condition configurations. From the results it appears that the configuration with more constrained points (8 P-P) does not provide a higher $M_{cr}$ for any lamination angle, but, $\theta$ equal to 60 provides a $M_{cr}$ lower than the configuration with 4 P-P. If isotropic panels are considered, $M_{cr}$ increases by increasing the number of pinched points; quite unexpected results could be obtained by varying boundary condition and panels lamination lay-out.

### D. Sandwich Panels Analysis

Classical shell models are not adequate for the analysis of sandwich panels. The critical flutter condition of a sandwich panel is investigated in this section. The panel is considered SS on the trailing and leading edges where the length is 0.5 m, and the width is 1 m. The two outer skins have a thickness of 0.0005 m and are made of aluminium alloy, $E = 75$ GPa, $\rho = 2700$ kg/m$^3$, and $\nu = 0.3$. The core has a thickness of 0.005 m and it is foam made with $E = 54$ MPa, $G = 23$ MPa, $\rho = 80$ kg/m$^3$, and $\nu = 0.17$. A $6 \times 6$ mesh was used. Four structural models were compared. The natural frequencies evaluated using the different structural models are reported in Table 5. The results obtained using the LD4 model are used as a reference solution. The results show that the ESL models need a high order displacement expansion to provide good accuracy. LW models provide better results and both considered models provide the same frequency value. Table 6 shows the results in terms of critical Mach number. The results highlight that ESL models are not very accurate.

### E. Cylindrical Panel Analysis

The aeroelastic analysis of cylindrical panels with different boundary conditions is carried out in this section. A square panel with an edge of 0.5 m and thickness equal to 0.002 m is considered. The material has $E = 75$ GPa, $\nu = 0.3$, and $\rho = 2700$ kg/m$^3$. A fully SS panel, a partially SS panel (only trailing and leading edge), a 4-point

**Table 6 Critical Mach number and flutter frequency for a sandwich panel, comparison between different structural models**

| | ED2 | ED4 | LD3 | LD4 |
|---|---|---|---|---|
| $M_{cr}$ | $2.61^{(38.1\%)}$ | $2.04^{(7.9\%)}$ | $1.92^{(1.6\%)}$ | 1.89 |
| $f_{cr}$ | $67.04^{(9.0\%)}$ | $62.65^{(1.9\%)}$ | $61.49^{(0.0\%)}$ | 61.49 |

and a 8-point pinched supported panel are considered. Each model was analysed using a ED3 theory. The results are reported in Fig. 4. The critical dynamic pressure, $\lambda$, of each model is reported for different curvature values. The curvature is represented by the dimensionless ratio $R/L$, where $R$ is the curvature radius and $L$ is the length of the leading edge of the panel. The results show that the critical flutter condition is affected to a great extent by the curvature and, as shown in the previous sections of this paper, by the boundary conditions. The critical dynamic pressure does not show a monotonic behaviour as the curvature increases (lower values of $R/L$), but rather it has several maximum and minimum values for all the constraint settings. This is a typical result of stability analysis in which different flutter modes can appear at different curvature values. To notice that, for $R/L = 2$, the configuration with 8 pinched points has a lower critical dynamic pressure than the model with 4 pinched points.

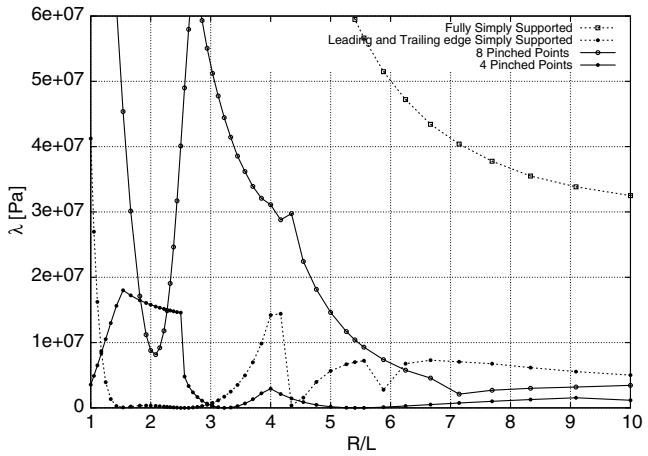


**Fig. 4 Effects of the curvature ($R/L$) on the critical dynamic pressure, $\lambda$. Different boundary conditions are considered: fully SS, partially SS, and pinched points supported panels.**

Figure 5 focuses attention on the behaviour of the 4 pinched point model. The evolution of the frequencies over a wide range of dynamic pressures is reported for $R/L$ equal to 2.43, 2.56, and 4.16. This figure highlights why 'steps' can be observed in Fig. 4. At $R/L = 2.56$, the instability arises due to the coupling between the fourth and the fifth frequencies, and it appears at about $5 \times 10^6$ Pa. A second instability appears at about $1.5 \times 10^7$ Pa. If the curvature is increased slightly ($R/L = 2.43$), the first instability disappears and the critical dynamic pressure abruptly increases from $5 \times 10^6$ Pa to a value of $1.5 \times 10^7$ Pa.

## IV. Conclusions

In this paper, an advanced shell element has been used to perform aeroelastic analyses of non-conventional panels. The structural model is based on a refined shell element developed using the Carrera Unified Formulation. The aerodynamic model is based on the linear piston theory. The advantages of the use of refined models in the aeroelastic analysis have been investigated. Isotropic, composite, and sandwich panels have been considered and different curvature values and boundary condition configurations are also analyzed.

The analysis of different boundary conditions focuses on the pinched point constraint configuration. The results have shown that, in the case of flat panels, the critical dynamic pressure increases with the number of pinched points at the edges. The effects of the boundary condition can be contrasted by the orientation of the fibers of the used composite panels, that is to say that tailoring play a crucial role in the aeroelastic design of panels. The use of refined models is recommended in the analysis of sandwich panels where the thickness deformation can not be neglected. Finally, panel curvature has a strong impact on aeroelastic instabilities and should be considered in the at early design stage.

In conclusion, the model presented in this paper appears to be suitable for aeroelastic analysis of conventional and unconventional panel configurations. More accurate aerodynamic models should be introduced in future works in order to extend the present model to both lower and higher speed regime.

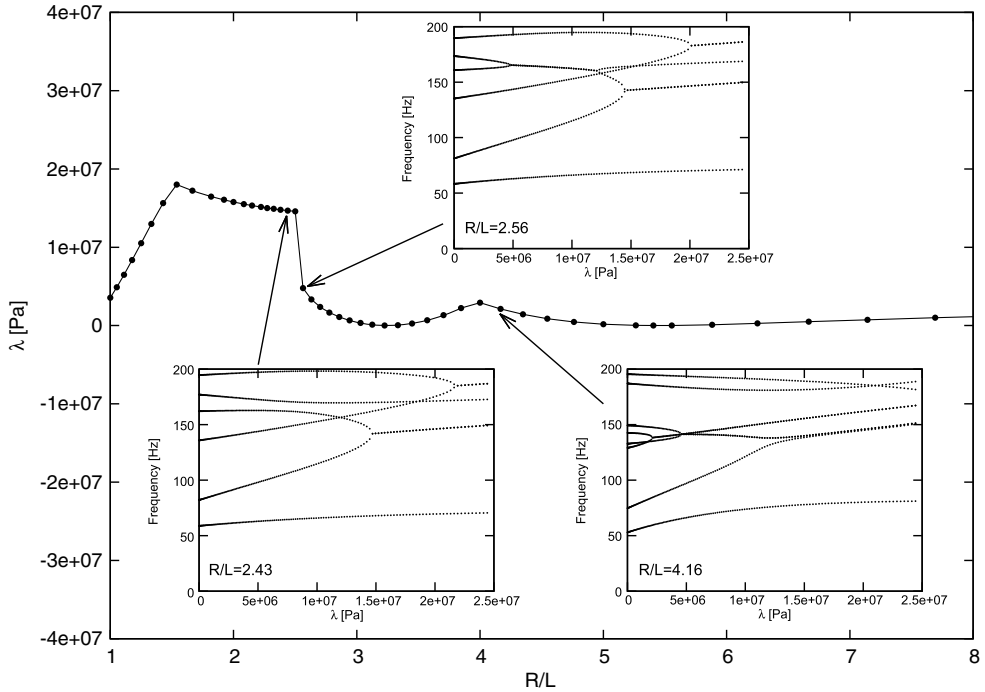


**Fig. 5 Effects of the curvature ($R/L$) on the critical dynamic pressure, $\lambda$, of a panel pinched in the four corners.**

## References


[1] Hayes, W., "A Buckled Plate in a Supersonic Stream," North American Aviation, Inc., Tech. Rept. AL-1029, May 1950.

[2] Miles, J., "Dynamic Chordwise Stability at Supersonic Speeds," North American Aviation, Inc., Tech. Rept. AL-1140, Oct. 1950.

[3] Shen, S., "Flutter of a Two-Dimensional Simply-Supported Uniform Panel in a Supersonic Stream," M.I.T., Dept. Aero. Eng. Office of Naval Research, Tech. Rept. N5 ori-07833, Cambridge, MA, Aug. 1952.

[4] Dowell, E. H., "Non-Linear Oscillation of a Fluttering Plate," *AIAA Journal*, Vol. 4, No. 7, 1966, pp. 1267–1275. doi:10.2514/3.3658

[5] Dowell, E. H., "Non-Linear Oscillation of a Fluttering Plate. II," *AIAA Journal*, Vol. 5, No. 10, 1967, pp. 1856–1862. doi:10.2514/3.4316

[6] Dowell, E. H., "Panel Flutter: A review of the Aeroelastic Stability of Plates and Shell," *AIAA Journal*, Vol. 8, No. 3, 1970, pp. 385–399. doi:10.2514/3.5680

[7] Ashley, H., and Zartarian, G., "Piston Theory—A New Aerodynamic Tool for the Aeroelastician," *Composites Structures*, 1956, pp. 1109–1118.

[8] Dowell, E. H., *Aeroelasticity of Plates and Shells*, Springer, New York, 1975, pp. 11–13.

[9] Lee, I., Lee, M. D., and Ho, K., "Supersonic Flutter Analysis of Stiffened Laminates Plates Subject to Thermal Load," *Journal of Sound and Vibrations*, Vol. 224, No. 1, 1999, pp. 49–67. doi:10.1006/jsvi.1998.2113

[10] Kariappa, B., Komashekar, B. R., and Shah, C. G., "Discrete Element Approach to Flutter of Skew Panels with In-Plane Forces Under Yawed Supersonic Flow," *AIAA Journal*, Vol. 8, No. 11, 1970, pp. 2017–2022. doi:10.2514/3.6040

[11] Shiau, L. C., and Lu, L. T., "Nonlinear Flutter of Two-Dimensional Simply Supported Symmetric Composite Laminated Plates," *Journal of Aircraft*, Vol. 29, No. 1, 1992, pp. 140–145. doi:10.2514/3.46137

[12] Dixon, I. R., and Mei, C., "Finite Element Analysis of Large-Amplitude Panel Flutter of Thin Laminates," *AIAA Journal*, Vol. 31, No. 4, 1993, pp. 701–707. doi:10.2514/3.11606

[13] Kouchakzadeh, M. A., Rasekh, M., and Haddadpoura, H., "Panel Flutter Analysis of General Laminated Composite Plates," *Composites Structures*, Vol. 92, No. 12, 2010, pp. 2906–2915. doi:10.1016/j.compstruct.2010.05.001

[14] Gordiner, R. E., and Visbal, M. R., "Development of a Three-Dimensional Viscous Aeroelastic Solver for Nonlinear Panel Flutter," *Journal of Fluids and Structures*, Vol. 16, No. 4, 2002, pp. 497–527. doi:10.1006/jfls.2000.0434

[15] Hashimoto, A., Aoyama, T., and Nakamura, Y., "Effects of Turbulent Boundary Layer on Panel Flutter," *AIAA Journal*, Vol. 47, No. 12, 2009, pp. 2785–2791. doi:10.2514/1.35786

[16] Carrera, E., and Zappino, E., "Aeroelastic Analysis of Pinched Panels in a Variable Supersonic Flow Changing with Altitude," *Journal of Spacecraft and Rockets*, Vol. 51, No. 1, 2013, pp. 187–199. doi:10.2514/1.A32363.

[17] Carrera, E., Zappino, E., Augello, G., Ferrarese, A., and Montabone, M., "Aeroelastic Analysis of Versatile Thermal Insulation Panels for Launchers Applications," *7th European Symposium on Aerothermodynamics for Space Vehicles* [CD-ROM], ESTEC, Noortwijk, The Netherlands, May 2011.

[18] Carrera, E., Zappino, E., Augello, G., Ferrarese, A., and Montabone, M., "Panel Flutter Analysis of Curved Panels for Launchers Applications," *Proceedings of the Spaces Access International Conferences*, ASTech Paris Region, Paris, France, Sept. 2011.

[19] Cinefra, M., and Carrera, E., "Shell Finite Elements with Different Through-the-Thickness Kinematics for the Linear Analysis of Cylindrical Multilayered Structures," *International Journal for Numerical Methods in Engineering*, Vol. 93, No. 2, 2013, pp. 160–182. doi:10.1002/nme.4377

[20] Carrera, E., Brischetto, S., and Nali, P., *Plates and Shells for Smart Structures: Classical and Advanced Theories for Modeling and Analysis*, John Wiley & Sons, New York, 2011.

[21] Cinefra, M., Chinosi, C., and Della Croce, L., "MITC9 Shell Elements Based on Refined Theories for the Analysis of Isotropic Cylindrical Structures," *Mechanics of Advanced Materials and Structures*, Vol. 20, No. 2, 2013, pp. 91–100. doi:10.1080/15376494.2011.581417

[22] Carrera, E., Cinefra, M., Petrolo, M., and Zappino, E., *Finite Element Analysis of Structures Through Unified Formulation*, John Wiley & Sons, New York, 2014, pp. 231–251.

[23] Krause, H., "Flattern flacher Schalen bei überschallanströmung," Ph.D. Dissertation, Inst. for Statics and Dynamics of Aerospace Structures, Univ. of Stuttgart, Stuttgart, 1998.


P. Gage
*Associate Editor*

# Queries

1. AU: Authors' information hav  en edited as per style. Please check and confirm.

2. AU: Please review the revised proof carefully to ensure your corre  s have been inserted properly and to your satisfaction.

3. AU: Table titles should be in a single phrase. If a table title  more than one sentence in it, the additional sentences should be converted to tablenotes. Please check and confirm.

4. AU: The final section must be called  nclusions".